Particulate solids modeling with discrete element methods

Stefan Luding
Particle Technology, Nanostructured Materials, DelftChemTech,
TU Delft, Julianalaan 136, 2628 BL Delft, The Netherlands
e-mail: s.luding@tudelft.nl

May 11, 2006

Abstract
Experiments and discrete element model (DEM) simulations of two-dimensional (2D) and three-dimensional (3D) granular materials are presented in ring shear cell geometries, undergoing slow deformation. The challenge is to quantitatively predict the flow behavior with the numerical model.

DEM is based on the particle positions, velocities and interaction forces. On the other hand, the flow behavior of powders is usually described using tensorial quantities like stress or strain. The velocity field and the deformation gradient will be used here for comparison.

The basic idea for DEM is to insert as little as possible information about the macroscopic flow behavior into the microscopic model and to see how much agreement with experiments can be achieved, since it is not desirable to fine-tune all material and system parameters anew for each different set-up. A predictive modeling tool will be adjusted to a small number of experiments and then will then lead to quantitative agreement with others.

1 Introduction

Powders and granular materials consist of many independent micro-particles with peculiar behavior, dependent on the conditions, when viewed from the macroscopic scale. Segregation, clustering, shear-band formation and arching are some examples for special powder flow behavior. The particle properties and interaction laws can be inserted into a discrete element model (DEM), which then follows the evolution of Newtons equations of motion for the dissipative, frictional, cohesive many-particle system under observation [1–3]. From the discrete picture, the goal is to obtain continuum constitutive relations as needed for industrial design. For this, methods and tools for a so-called micro-macro transition [4] were developed recently. The "microscopic" simulations of small samples (representative volume elements) can be used to derive macroscopic constitutive relations needed to describe the material within the framework of a continuum theory.

However, every simulation method relies on experiments for validation. Thus, in the following, rather simple two- and three-dimensional ring-shear test simulations will be compared to experimental results. In 2D, the grains are disks confined between flat top- and

bottom-planes and an inner, rotating wheel and a fixed outer ring. Shear band localisation is observed at the inner wheel [5–7], with an exponential decay of the velocity field away from the inner boundary. In 3D, the particles are spheres confined within two cylindrical walls and a bottom with a slit. According to the experimental design, here the outer wall is moving and a part of the bottom is rotating with it [8, 9]. The shear band is initiated at the bottom slit and its velocity field is well approximated by an error-function [9, 10]. The simulation results are compared to experimental data and quantitative agreement is found, with deviations of the order of 20 per-cent. We discuss the quantitative agreement/disagreement, give possible reasons, and outline further research perspectives.

1.1 The Soft Particle Molecular Dynamics Method

Information about the behavior of granular media can be obtained from the discrete element method (DEM) or from molecular dynamics (MD) [1, 4, 7, 10, 11]. Note that both methods are identical in spirit, however, different groups of researchers use these (and also many other) names. Particle positions, velocities and interaction forces are sufficient to integrate Newtons equations of motion. Conceptually, the MD or DEM method has to be separated from the hard sphere event-driven (ED) molecular dynamics, and also from the so-called Contact Dynamics (CD) [10], which are not discussed here in detail. Only the main difference is mentioned: the particles are soft, deformable in the framework of DEM while they are rigid in the other two methods. The effect of excluded volume and repulsion is thus intrinsic to all models, however, the non-linear details of information propagation on the contact level cannot be typically included in ED or CD. For many quasi-static situations this is not relevant but, e.g., for sound-propagation these details are of eminent importance.

1.2 Discrete Particle Model

The elementary units of powders are mesoscopic grains, which deform under stress. Since the realistic modeling of the deformations of the particles is much too complicated, we relate the interaction force to the overlap δ of two particles. Note that the evaluation of the inter-particle forces based on the overlap may not be sufficient to account for the inhomogeneous stress distribution inside the particles. Consequently, our results presented below are of the same quality as the simple assumptions about the force-overlap relation [7, 12].

Only the simplest linear spring-dashpot force laws in normal direction and a Coulomb sliding spring-dashpot in tangential direction will be used in this study, so that we rather than going into detail, we refer to the basic literature [13].

If all forces $\boldsymbol{f}_i$ acting on the particle i, either from other particles, from boundaries or from external forces, are known, the problem is reduced to the integration of Newtons equations of motion for the translational and rotational degrees of freedom. The equations of motion are thus a system of $\mathcal{D}+\mathcal{D}(\mathcal{D}-1)/2$ coupled ordinary differential equations to be solved in $\mathcal{D}$ dimensions per particle. With tools from numerical integration, as nicely described in textbooks as [14, 15], this is a straightforward exercise. The typically short-ranged interactions in granular media, allow for a further optimization by using linked-cell or alternative methods in order to make the neighborhood search efficient enough to allow simulations with about 10^5 particles on a single personal computer.

2 The 2D Couette ring shear cell

The physical system discussed here was studied experimentally and numerically [5–7, 16–20]. In the following, the experimental set-up is reviewed and differences between the simulations and the physical system are discussed, concerning boundary and initial conditions. The steady state velocity profiles are examined in detail.

2.1 Experimental Setup and Procedure

The experimental setup and results are discussed in more detail in Refs. [7, 16, 19, 20]. The apparatus, as sketched in Fig. 1, consists of (A) an inner rotating wheel (with radius $R = 10.32\,\mathrm{cm}$), and (B) an outer, stationary ring with radius $R_o = 25.24\,\mathrm{cm}$ confined by (C) planetary gears. In the experiments, a bimodal distribution of disks (D) is used, with about 400 larger disks of diameter $d_{\mathrm{large}} = 0.899\,\mathrm{cm}$, and about 2500 smaller disks of diameter $d_{\mathrm{small}} = 0.742\,\mathrm{cm}$. An inhomogeneous distribution is useful, since it limits the formation of hexagonally ordered regions over large scales, even though there might still be some short range order [21]. We use the diameter of the smaller disks, $d = d_{\mathrm{small}}$, as the characteristic length scale for rescaling.

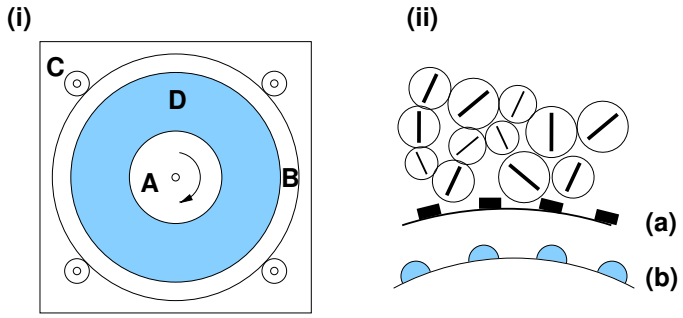

Figure 1: (i) Schematic top view of the experimental setup, (ii) schematic drawing of the disks close to the shearing wheel, (a) experimental realization of the walls, and (b) realization of the walls in the simulation.

The boundary conditions are chosen to mimic those in the experiment. However, the "teeth" used on the inner and outer ring of the experiment are replaced by small disks with diameter $d_{\mathrm{wall}} = 0.25\,\mathrm{cm}$, see Fig. 1. While the variation in height is thus of the same order as in the experiments, to roughness (or sharpness) of the walls is smaller in the simulations.

The experimental walls are fixed, corresponding to a *constant volume boundary condition*. All particles are inserted into the system and the shear is applied via the inner wall for several rotations, before averages in the supposed steady state are taken. The shearing rate is set by the angular frequency Ω, the rotation rate of the inner wheel. In the experiments, rate-independency was found for $0.0029\,\mathrm{s}^{-1} \leq \Omega \leq 0.09\,\mathrm{s}^{-1}$, while some simulations in the range $0.01\,\mathrm{s}^{-1} \leq \Omega \leq 1.0\,\mathrm{s}^{-1}$ showed clear rate independence for the slower shearing rates. Averages in the simulations are performed after about three rotations starting at $t = 180\,\mathrm{s}$, and extending over three rotations, until $t = 360\,\mathrm{s}$. Averages in the experiments are taken after much longer initialization time and also over many more rotation rounds.

The mean packing fraction $\bar{\nu}$ (fractional area occupied by disks) is varied over the range $0.797 \leq \bar{\nu} \leq 0.837$ in the simulations. For too low density, in the *sub-critical* regime, $\bar{\nu} \leq 0.8$, the particles are pushed away from the inner wall and lose contact, so that shearing stops. For too high densities, $\bar{\nu} \geq 0.817$, dilation and thus shear are hindered and the system becomes *blocked*, i.e. the inner particles slip on the inner wall and no shearband develops. Thus, the range of densities that allow for the steady state shear flow is extremely narrow. Taking or leaving a small or large particle leads to a density change of 0.00026 or 0.00038, respectively. The densities (area fractions) given have three digit accuracy in order to allow a distinction between runs differing by only a few particles. However, the error in the experimental density values is much larger (at least ± 0.02). Furthermore, a density-shift was introduced in order to match simulation and experimental results, see Ref. [7], to account for systematic deviations in density determination.

2.2 Similarity between Simulation and Experiment

The parameters used in the model were chosen to match the experiments as reasonably as possible. Specifically, the radii, static friction coefficient and density of the particles, and the size of the container match the experimental values. Still, there remain some nominally modest differences between the experiment and the simulation, which may lead to differences between results for the two realizations. The main differences are:

- The numerical code used here only accounts for a very weak viscous friction with the bottom plate. Furthermore, friction reduction in the experiment is achieved by fine powder on the bottom plate, which is too complicated to be included into the model.
- Related to the disk shape of the particles is a possible small tilt of the real particles out of plane of observation, connected to increased tangential and frictional forces due to increased, artificial, normal forces.
- Particle-wall and particle-particle contacts are modeled by simple linear force laws and thus, possibly, do not reproduce reality to the extent desired. Some test simulations with more realistic non-linear interaction laws did not show considerable differences though. The particles in the experiments are deformed considerably while the model particles only overlap.
- In the experiment the walls are never as perfectly round as in the simulations, which in the end leads to a slightly larger effective radius of the inner wall and to intermittency – sometimes nothing moves, until a bump in the wall finds particles to touch.
- The initial state is prepared differently for the experiments and the simulations. The starting state in the experiments is a nearly uniform density at the mean packing fraction, $\bar{\nu}$. The initial state of the simulation is an initially dilated state that is then compressed.

2.3 Velocity profiles

With varying density, the velocity profiles (and the spin profiles – not shown here) change also. In Fig. 2, data for the scaled velocity are shown for different $\bar{\nu}$, from both experiment and simulation. The profiles of $v_\theta/(\Omega R)$, show a roughly *exponential decay*, although there is some

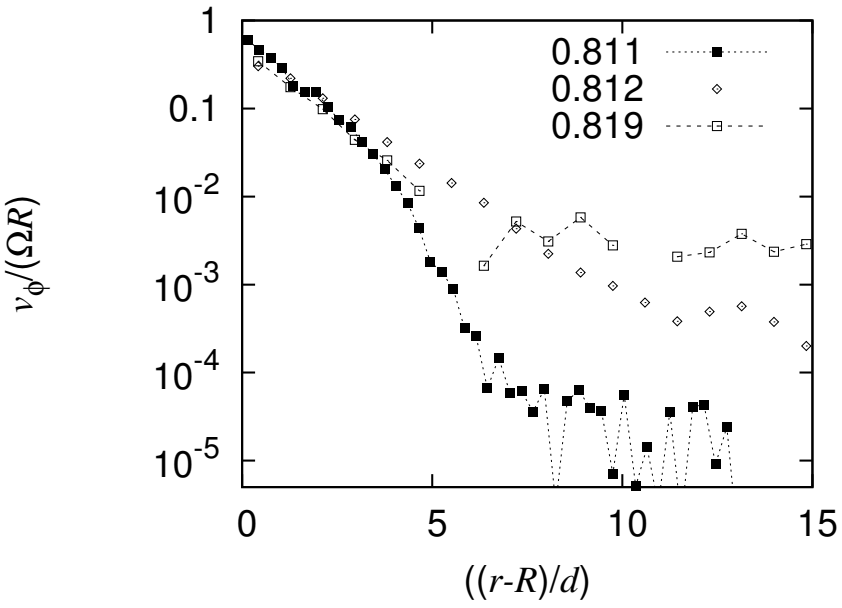

Figure 2: Velocity profiles for selected packing fractions $\bar{\nu}$ as given in the inset. The solid and open symbols denote experimental and simulational data, respectively.

clear curvature in the experimental data at the outer edge of the shear zone, $(r-R)/d \approx 5-7$, where the saturation level is reached. This *saturation level* of fluctuations of the velocity is at a higher level in the simulations, possibly due to the longer averaging in experiments, due to systematically larger shear rates in simulations, or even due to contact model details.

While the velocity decay (the width of the shear band) is in quantitative agreement over some range of densities, the wall-slip, i.e., the velocity close to the wall, is typically much less accurately predicted by the model – not astonishing given the geometrically different model walls. Values of $v_0/(\Omega R) = 1$, with $v_0 = v_\theta(r = R)$, would correspond to perfect shear in the sense that the particles are moving with the wall without slip. For high densities, the agreement between experiments and simulations is reasonable, but for low densities, the magnitude of the velocities differs strongly. This may be due to either the differences in bottom- or wall-friction, or due to more irregular and differently shaped walls in the experiments, causing more intermittency and thus reduced mean velocities. For the case of low densities, the bottom friction and wall effects are expected to be most important, since in this regime, the particle-particle interaction forces are at their weakest, and intermittent behavior is relatively strong.

When one examines the velocity- and spin-distributions in more detail, close to the inner wall, an alternating rolling is observed from the wall outwards – layer by layer. Furthermore, the data indicate non-rotating particles at rest and particles rolling over the shearing innner wall. With increasing density, more and more particles are found in the latter state [5, 7].

In summary, both simulations and experiments show rate-independence within the statistical errors, and the range of smaller rates studied. Good agreement between simulation and experiment was found for the density profiles (modulo an overall density shift – data not shown here) associated with dilatancy and the formation of a shear band next to the inner shearing wheel with a characteristic width of about 5 to 6 particle diameters – in quantitative

agreement with experiments. The velocity decay is exponential and so is, roughly, the velocity gradient. However, the simulations did neither capture the density dependence of the experimental velocity profiles for small densities, nor some details of the shape, especially at the outer edge of the shear band. Most sensible appears the boundary condition: the wall-slip is only qualitatively following the experimental observations. In this regard, further exploration of the role played by roughness of the shearing surface and the effect of the particle-bottom friction are necessary. The former can lead to more intermittent behavior, whereas the latter might explain the velocity-drop at the outer edge of the experimental shear band.

3 Ring shear cell simulation in 3D

The simulation in this section models a ring-shear cell experiment, as recently proposed [8–10]. The interesting observation in the experiment is a universal shear zone, initiated at the bottom of the cell and becoming wider and moving inwards while propagating upwards in the system.

3.1 Model system

In order to save computing time, only a quarter of the ring-shaped geometry is simulated. The walls are cylindrical, and are rough on the particle scale due to some (about 3 per-cent of the total number) attached particles [10]. The outer cylinder wall with radius R_o, and part of the bottom $r > R_s$ are rotating around the symmetry axis, while the inner wall with radius R_i, and the attached bottom-disk $r < R_s$ remain at rest. In order to resemble the experiment, the geometry data are $R_i = 0.0147\,\mathrm{m}$, $R_s = 0.085\,\mathrm{m}$, and $R_o = 0.110\,\mathrm{m}$. Note that the small R_i value is artificial, but it does not affect the results for small and intermediate filling heights.

The slit in the bottom wall at $r = R_s$ triggers a shear band. In order to examine the behavior of the shear band as function of the filling height H, this system is filled with 6000 to 64000 spherical particles with mean radius $\langle a \rangle = 1.0\,\mathrm{mm}$ and radii range $0.5\,\mathrm{mm} < a < 1.5\,\mathrm{mm}$. The particles are forced towards the bottom by gravity and are kept inside the system by the cylindrical walls.

3.2 Material and system parameters

The simulations run for 25 s with a rotation rate $f_o = 0.01\,\mathrm{s}^{-1}$ of the outer cylinder, with angular velocity $\Omega_o = 2\pi f_o$. For the average of the displacement, only times $t > 10\,\mathrm{s}$ are taken into account. Within the averaging accuracy, the system seemingly has reached a quasi-steady state after about 8 s. Two realizations with different filling height are displayed in Fig. 3, both as top- and front-view.

3.3 Shear deformation results

From the top-view, it is evident that the shear band moves inwards with increasing filling height, and it also becomes wider. From the front-view, the same information can be evidenced and, in addition, the shape of the shear band inside the bulk is visible: The inwards displacement happens deep in the bulk and the position of the shear band is not changing a lot closer to the surface.

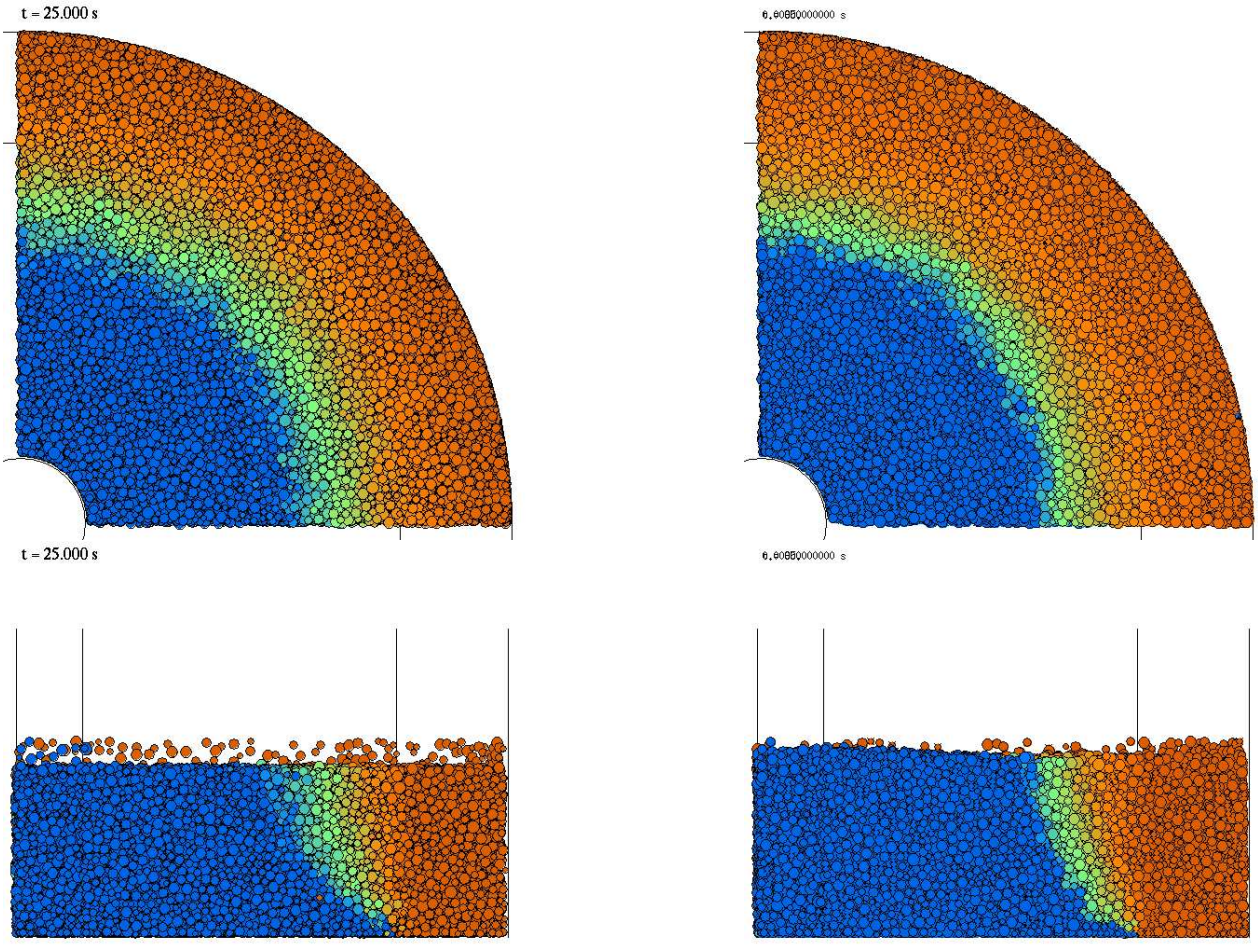

Figure 3: Snapshots from simulations with different friction coefficient, but the same number of particles, seen from the top and from the front. The particle number is $N = 34518$ without friction $\mu = 0$ (Left) and with friction $\mu = 0.4$ (Right). The colors blue, green, orange and red denote particles with $r\,\mathrm{d}\phi \leq 0.5\,\mathrm{mm}$, $r\,\mathrm{d}\phi \leq 2\,\mathrm{mm}$, $r\,\mathrm{d}\phi \leq 4\,\mathrm{mm}$, and $r\,\mathrm{d}\phi > 4\,\mathrm{mm}$, i.e. the displacement in tangential direction per second, respectively. The filling heights in these simulations are $H \approx 0.037\,\mathrm{m}$ (Left) and $H \approx 0.039\,\mathrm{m}$ (Right).

In order to allow for a more quantitative analysis of the shear band, both on the top and as function of depth, we perform fits with the universal shape function proposed in Ref. [8]: $v_\varphi(r)/(r\Omega_o) = A + B\,\mathrm{erf}\left(\frac{r-R_c}{W}\right)$ where A and B are dimensionless amplitudes $A \approx B \approx 0.51 \pm 0.01$, (somewhat smaller for the frictional case), R_c is the center of the shearband, and W its width. Note that R_c corresponds to the maximum of the velocity gradient.

The fits to the simulations confirm the experimental findings in so far that the center of the shear band, as observed on top of the material, moves inwards with a $R_c \propto H^{5/2}$ behavior, see Ref. [10], and that the width of the shear band increases almost linearly with H. Quantitatively speaking, the agreement is 80%, i.e., the simulations without friction lead to a somewhat slower shift of the shearband inwards. For filling heights larger than $H \approx 0.05\,\mathrm{m}$, deviations from this behavior are observed, because the inner cylinder is reached and thus sensed by the shearband. Slower shearing does not affect the center position, but reduces

slightly the width.

The packing is considerably less dense in the presence of friction, which leads to a larger filling height. Furthermore, the filling height varies strongly in radial direction: it is minimal where the velocity gradient is largest.

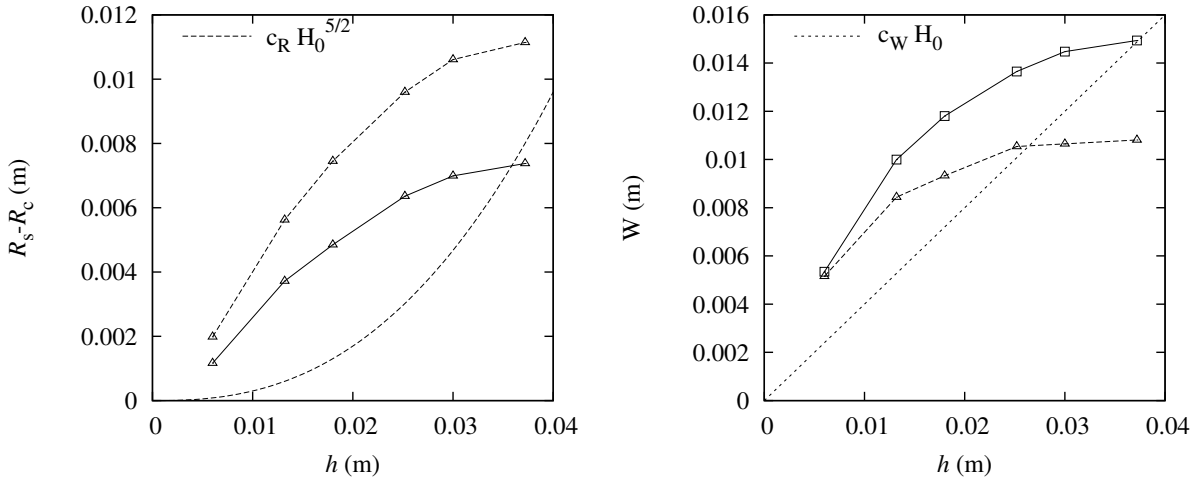

Figure 4: (Left) Distance of the bulk shearband center from the slit and, (Right) width of the shearband, both plotted against the height h for the simulations from Fig. 3 with the coefficients of friction $\mu = 0.0$ (squares) and $\mu = 0.4$ (triangles). The lines indicate the position of the center and the width as observed at the top from frictionless simulations [10].

Like in the experiments, the behavior of the shearband within the bulk, see Fig. 4 (symbols), deviates qualitatively from the behavior seen from the top (lines). Instead of a slow motion of the shear band center inwards, the shear band rapidly moves inwards at small heights h, and reaches a saturation distance with small change closer to the surface. Again, a slower rotation does not affect the center but reduces the width (data not shown here) [10]. Notably, the presence of friction does not affect the qualitative behavior but the center position and the width: The shear band with friction moves inwards more rapidly and is considerably narrower than without friction.

This example of a peculiar ring shear cell simulation in 3D has shown, that even without the more complicated details of fancy interaction laws, experiments can be reproduced quantitatively with 80% agreement. The simulations with friction lead towards even better agreement but further studies are needed here.

4 Conclusion

Some examples of ring shear cell simulations in both 2D and 3D showed qualitative and even quantitative agreement with experiments. Because the model is much less involved than reality – many details as discussed above are not catched by the simulations – there is better agreement in the denser regimes for both 2D and 3D. The error margin is about 20 per-cent – not so bad a result given the enormous number of differences between model and experiment.

In conclusion, molecular dynamics methods are a helpful tool for the understanding of granular systems because they allow insight on the particle and the contact level. The

qualitative approach of the early years has now developed into the attempt of a quantitatively predictive modeling of the diverse modes of complex behavior in granular media, powders and bulk solids. This should eventually lead to elaborate constitutive models for quasi-static, dense systems with a micro-based understanding.

Acknowledgements

We acknowledge the financial support of several funding institutions that supported the reviewed research, the Deutsche Forschungsgemeinschaft (DFG), and the Stichting voor Fundamenteel Onderzoek der Materie (FOM), financially supported by the Nederlandse Organisatie voor Wetenschappelijk Onderzoek (NWO). Furthermore, also the helpful discussions with all those persons that contributed to these results are acknowledged.

References

[1] H. J. Herrmann, J.-P. Hovi, and S. Luding, editors. *Physics of dry granular media - NATO ASI Series E 350*, Dordrecht, 1998. Kluwer Academic Publishers.

[2] Y. Kishino, editor. *Powders & Grains 2001*, Rotterdam, 2001. Balkema.

[3] S. Luding, M. Lätzel, and H. J. Herrmann. From discrete element simulations towards a continuum description of particulate solids. In A. Levy and H. Kalman, editors, *Handbook of Conveying and Handling of Particulate Solids*, pages 39–44, Amsterdam, The Netherlands, 2001. Elsevier.

[4] P. A. Vermeer, S. Diebels, W. Ehlers, H. J. Herrmann, S. Luding, and E. Ramm, editors. *Continuous and Discontinuous Modelling of Cohesive Frictional Materials*, Berlin, 2001. Springer. Lecture Notes in Physics 568.

[5] M. Lätzel, S. Luding, and H. J. Herrmann. Macroscopic material properties from quasi-static, microscopic simulations of a two-dimensional shear-cell. *Granular Matter*, 2(3):123–135, 2000. e-print cond-mat/0003180.

[6] M. Lätzel, S. Luding, and H. J. Herrmann. From discontinuous models towards a continuum description. In P. A. Vermeer, S. Diebels, W. Ehlers, H. J. Herrmann, S. Luding, and E. Ramm, editors, *Continuous and Discontinuous Modelling of Cohesive Frictional Materials*, pages 215–230, Berlin, 2001. Springer.

[7] M. Lätzel, S. Luding, H. J. Herrmann, D. W. Howell, and R. P. Behringer. Comparing simulation and experiment of a 2d granular couette shear device. *Eur. Phys. J. E*, 11(4):325–333, 2003.

[8] D. Fenistein and M. van Hecke. Kinematics – wide shear zones in granular bulk flow. *Nature*, 425(6955):256, 2003.

[9] D. Fenistein, J. W. van de Meent, and M. van Hecke. Universal and wide shear zones in granular bulk flow. *Phys. Rev. Lett.*, 92:094301, 2004. e-print cond-mat/0310409.

[10] S. Luding. Molecular dynamics simulations of granular materials. In H. Hinrichsen and D. E. Wolf, editors, *The Physics of Granular Media*, pages 299–324, Weinheim, Germany, 2004. Wiley VCH.

[11] S. Luding. Micro-macro transition for anisotropic, frictional granular packings. *Int. J. Sol. Struct.*, 41:5821–5836, 2004.

[12] S. Luding. Granular media: Information propagation. *Nature*, 435:159–160, 2005.

[13] S. Luding. Collisions & contacts between two particles. In H. J. Herrmann, J.-P. Hovi, and S. Luding, editors, *Physics of dry granular media - NATO ASI Series E350*, page 285, Dordrecht, 1998. Kluwer Academic Publishers.

[14] M. P. Allen and D. J. Tildesley. *Computer Simulation of Liquids*. Oxford University Press, Oxford, 1987.

[15] D. C. Rapaport. *The Art of Molecular Dynamics Simulation*. Cambridge University Press, Cambridge, 1995.

[16] C. T. Veje, D. W. Howell, R. P. Behringer, S. Schöllmann, S. Luding, and H. J. Herrmann. Fluctuations and flow for granular shearing. In H. J. Herrmann, J.-P. Hovi, and S. Luding, editors, *Physics of dry granular media - NATO ASI Series E 350*, page 237, Dordrecht, 1998. Kluwer Academic Publishers.

[17] S. Schöllmann. Simulation of a two-dimensional shear cell. *Phys. Rev. E*, 59(1):889–899, 1999.

[18] H. J. Herrmann and S. Luding. Modeling granular media with the computer. *Continuum Mechanics and Thermodynamics*, 10:189–231, 1998.

[19] D. Howell, R. P. Behringer, and C. Veje. Stress fluctuations in a 2d granular Couette experiment: A continuous transition. *Phys. Rev. Lett.*, 82(26):5241–5244, 1999.

[20] D. W. Howell, R. P. Behringer, and C. T. Veje. Fluctuations in granular media. *Chaos*, 9(3):559–572, 1999.

[21] S. Luding. Liquid-solid transition in bi-disperse granulates. *Advances in Complex Systems*, 4(4):379–388, 2002.